Am J Cancer Res 2022;12(9):4361-4372
www.ajcr.us /ISSN:2156-6976/ajcr0144797

Original Article

CircMYH9 increases KPNA2 mRNA stability to promote hepatocellular carcinoma progression in an EIF4A3-dependent manner

Jinguo Xia[1*], Chen Wu[1*], Yanhui Tang[2*], Junwei Tang[3], Deming Zhu[1], Feihong Zhang[1], Zhenggang Xu[1], Dongwei Sun[1], Zhongming Tan[1], Han Zhuo[1]

[1]Hepatobiliary Center, The First Affiliated Hospital of Nanjing Medical University, Nanjing, Jiangsu, P. R. China; [2]Qidong Hospital of Traditional Chinese Medicine, Nantong, Jiangsu, P. R. China; [3]General Surgery, The First Affiliated Hospital of Nanjing Medical University, Nanjing, Jiangsu, P. R. China. [*]Equal contributors.

Received June 16, 2022; Accepted September 1, 2022; Epub September 15, 2022; Published September 30, 2022

Abstract: Hepatocellular carcinoma (HCC) is the most commonly diagnosed cancer worldwide with a high incidence of recurrence and metastasis; however, the molecular mechanisms underlying HCC development remain to be fully understood. In this study, we identified circMYH9 as an important regulator of HCC. Overexpression of circMYH9 induced, while knockdown of circMYH9 inhibited, the proliferation, migration, and invasion of HCC cells. Mechanistically, circMYH9 bound to eukaryotic translation initiation factor 4A3 (EIF4A3) and increased karyopherin subunit alpha 2 (KPNA2) mRNA stability. circMYH9 knockdown in HCC cells reduced the stability of KPNA2 mRNA. Importantly, circMYH9 regulation of HCC required the activity of KPNA2. In support with this, circMYH9 level was positively correlated with the expression of KPNA2 in HCC patient samples. Taken together, our study was the first to uncover the oncogenic role of circMYH9 in HCC and further elucidated the functional mechanism of circMYH9 by interacting with EIF4A3 to increase KPNA2 mRNA stability. Our findings might provide a novel potential target for the diagnose and treatment of HCC.

Keywords: CircMYH9, EIF4A3, mRNA stability, hepatocellular carcinoma, KPNA2

Introduction

HCC is the six most common cancer worldwide, accounting for almost 90% of liver cancer [1]. Genetic susceptibility, chronic hepatitis B virus (HBV) infection, lifestyle, and non-alcohol-related steatohepatitis (NASH) have been recognized as the risk factors associated with HCC [2, 3], which makes HCC a clinically and biologically heterogeneous disease. Therefore, it is imperative to identify new molecular targets for the diagnose and treatment of HCC.

circular RNAs (circRNAs) belong to the family of non-coding RNAs which include microRNAs and long non-coding RNAs [4]. Like other non-coding RNAs, almost all circRNAs are originated from their precursor mRNAs (pre-mRNAs). RNA polymerase II (Pol II) can catalyze splicing event and a series of other processes [5]. Most circRNAs are produced from exons through back-splicing to form the junction site, which is different from the formation of linear RNAs [6]. circRNAs are classified into different types according to their genomic origins, including exonic, intronic, and intergenic circRNAs [5]. Different types of circRNAs have different intracellular location preferences. For instance, exonic circRNAs are mainly localized in the cytoplasm [7-9]. Furthermore, pre-tRNAs can also be spliced to form the tRNA intronic circRNAs in their intergenic regions [10].

circRNAs are important biological molecules and play crucial roles in cancer development through regulating many cellular processes, including microRNA sponges [11], protein sponges or scaffolds [12], translation templates [13], and gene expression [8]. For example, circRPN2 inhibits aerobic glycolysis and metastasis in HCC [14]. circRNA_069718 regulates the expression of Wnt/β-catenin pathway-related ge-

Table 1. The clinicopathological features of HCC patients (n = 15)

Patients	n (%)
Age (years)	
< 60	9 (60.0)
≥ 60	6 (40.0)
Gender	
Male	9 (60.0)
Female	6 (40.0)
T stage	
T1-T2	11 (73.3)
T3-T4	4 (36.7)
Regional lymph node metastasis	
Yes	3 (20.0)
No	12 (80.0)
Distance metastasis	
Yes	5 (33.3)
No	10 (66.7)
Tumor size	
< 5 cm	8 (53.3)
≥ 5 cm	7 (46.7)

nes, e.g., β-catenin, c-myc, and cyclin D1 [15]. In our current study, we found that circMYH9 was upregulated in HCC tissues and acted as an oncogene to promote the proliferation, migration, and invasion of HCC cells. Moreover, circMYH9 could increase karyopherin subunit alpha 2 (KPNA2) mRNA stability by binding to eukaryotic translation initiation factor 4A3 (EIF4A3), demonstrating the potential of circMYH9 as a novel target for the diagnose and treatment of HCC.

Materials and methods

HCC tissue samples

A Total of 15 paired tumor and non-tumor tissues of HCC patients were collected from Hepatobiliary Center, The First Affiliated Hospital of Nanjing Medical University, from 2019 to 2021. All tissue specimens were snap-frozen and stored in liquid nitrogen for further analysis. The clinical information of these samples was summarized in **Table 1**. This study was approved by the Ethics Committee of The First Affiliated Hospital of Nanjing Medical University. Written informed consent form was obtained from all patients.

Cell culture and transfection

Human HCC cell line Huh-7 was purchased from the Chinese Academy of Sciences (Shanghai, China), cultured in Dulbecco's modified Eagle's medium (DMEM) (Gibco, USA) supplemented with 10% fetal bovine serum (FBS) (Gibco, USA), and maintained in a 37°C humidified incubator with 5% CO_2. si-circMYH9, si-EIF4A3, si-KPNA2 and scramble siRNA as negative control (NC) were purchased from Genepharm (Shanghai, China). circMYH9-overexpressing plasmid was constructed by cloning circMYH9 into lentiviral vector pLCDH-ciR (GENEWIZ, Shanghai, China). Cell transfection using Lipofectamine 3000 (Invitrogen, Shanghai, China) was performed following the manufacturer's instruction.

RNA extraction and quantitative real-time PCR (qRT-PCR)

Total RNA was isolated by TRIzol reagent (Invitrogen, USA). SYBR Green qPCR SuperMix Kit (Vazyme, Nanjing, China) was used for qRT-PCR. Data were normalized to GAPDH according to the manufacturer's protocol. Primers used for qRT-PCR were as follows: circMYH9 (F: 5'-CTCATGCCCTCCAGCCAG-3', R: 5' GGTCCAAGGCCAGCTCTG-3'); GAPDH (F: 5'-TGCACCACCAACTGCTTAGC-3', R: 5'-GGCATGGACTGTGGTCATGAG-3'); KPNA2 (F: 5'-CTGCCCGTCTTCACAGATTCA-3', R: 5'-GCGGAGAAGTAGCATCATCAGG-3').

mRNA stability assay by using actinomycin D

Huh-7 cells were treated with 2 mg/mL actinomycin D (Merck, Germany) for different times to block transcription. The following RNA extraction and examination by qRT-PCR were performed as described above.

Fluorescence in situ hybridization (FISH) assay

FISH assay was carried out by using a FISH kit from GenePharma (Shanghai, China). Specific probes for circMYH9 were synthesized by GenePharma (Shanghai, China). Briefly, cells were fixed with 4% paraformaldehyde, permeabilized with 0.5% Triton X-100, and incubated with circMYH9 probes overnight. Nuclei were counterstained with DAPI. Images were captured with fluorescence microscope.

CCK8 assay

About 2,000 of transfected Huh-7 cells were seeded in 96-well plates. A CCK8 assay kit (Sigma, USA) was used to determine cell viability. The absorbance was measured by a microplate reader at the indicated time points.

Wound healing assay

Transfected Huh-7 cells were grown in six-well plates to 90% confluence. A 200 μl sterile pipette tip was used for wound scratching. The cells were photographed by microscope at time 0 h. Images were taken again at 24 h after scratching in the same spots for comparison. The rate of wound closure was calculated. All measurements were repeated three times.

Transwell assay

Transwell invasion assay was conducted in 24-well chamber with Matrigel coated membrane insert (Millipore, USA). Briefly, cell suspension was added to the upper chamber of transwell inserts. After incubation for 24 h, the cells that have invaded to the underside of chamber were stained. The number of penetrating cells was determined under the inverted microscope and quantified.

RNA pull-down assay

An RNA pull-down assay kit (BersinBio, Guangzhou, China) was used to detect the RNA-binding proteins (RBPs) of circMYH9. The biotin-labeled probe targeting circMYH9 was designed and synthesized by GenePharma (Shanghai, China). The specific probes were incubated with cell lysates to form the RNA-protein complex, and streptavidin-conjugated magnetic beads were used to pull down the protein for immunoblotting.

RNA immunoprecipitation (RIP) assay

RIP assays were conducted by using a RIP assay kit (BersinBio, Guangzhou, China) following the manufacturer's instruction. Briefly, cell lysates were incubated with magnetic beads and anti-EIF4A3 or anti-IgG as negative control (Proteintech, China). The enriched RNAs were analyzed by qRT-PCR.

Western blotting analysis

Briefly, cells were lysed with RIPA lysis buffer, and the cells lysates were cleared by centrifugation. The supernatants were collected, and protein concentration was quantified by BCA kit. Western blot was performed following the standard protocol. Antibodies against Cyclin D1, Cyclin E2, EIF4A3 and GAPDH were purchased from Cell Signal Technology (CST, USA). The signal was developed by chemiluminescent substrate (ECL; Millipore) and visualized by Image Lab. Image Lab software was used to analyze the results.

Xenograft tumor model

Six-week-old male nude mice (BALB/c background) were randomly divided into two groups, control group and experimental group, for our in vivo xenograft tumor study. First, Huh-7 cells were transfected with control vector or circMYH9 overexpressing plasmid. Then, the vector- or circMYH9-expressing Huh-7 cells were collected and subcutaneously injected into the flank of the control group mice or into the flank of the experimental group mice, respectively. The Huh-7 cell-derived tumor growth was monitored for 5 weeks, and, at the end of the experiment, mice imaging was performed, and the tumor weight was examined. All animal experiments were approved by the Committee on the Ethics of Animal Experiments of Nanjing Medical University.

Statistical analysis

All experiments were carried out in $n \geq 3$ of biological replicates. Statistical analyses were performed by SPSS IBM 20.0. The *P*-values were determined by using t test (student's t test) or ANOVA (Analysis of Variance). Values of $P < 0.05$ were considered statistically significant, and values of $P < 0.01$ were considered extremely significant (*P < 0.05; **P < 0.01; ***P < 0.001). All data in the graphs were presented as mean ± SD.

Results

Higher circMYH9 expression in HCC tissues

To explore differentially expressed circRNAs in HCC, we performed bioinformatics analysis by using different GEO databases, including GSE138734 and GSE122482 (**Figure 1A** and **1B**). A total of 14 upregulated circRNAs and 11

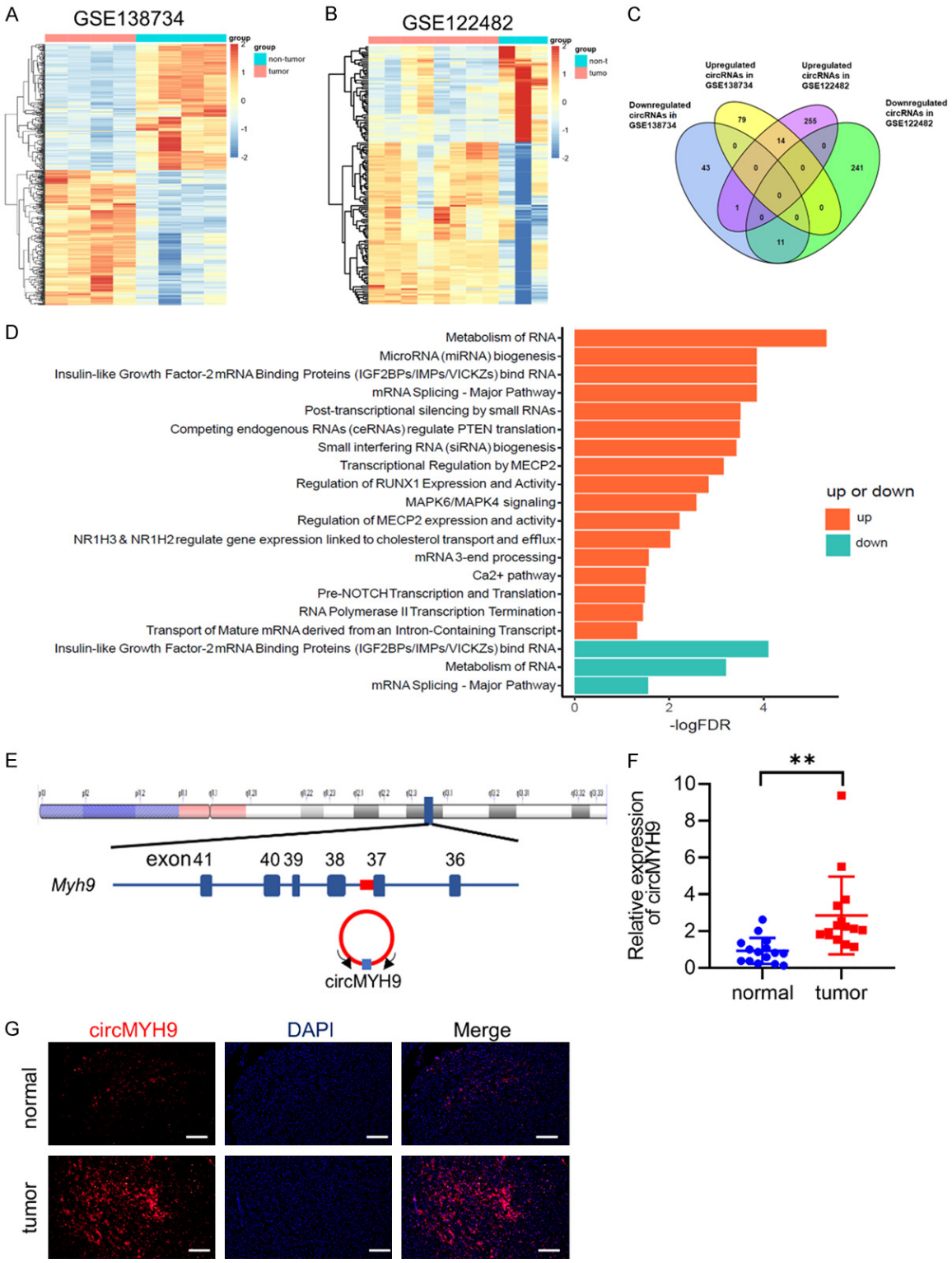

Figure 1. Elevated CircMYH9 expression in HCC tissues. (A, B) Heat maps of differentially expressed circRNAs in HCC tissues and non-tumor tissues obtained from GSE138734 and GSE122482. (C) The intersected differentially expressed circRNAs from two GEO databases were shown in venn diagram. (D) KEGG pathways in differentially expressed circRNAs. (E) The schematic diagram of MYH9 gene location and circMYH9 formation. (F, G) The expression of circMYH9 in 15 paired HCC tumor and non-tumor tissues was evaluated by qRT-PCR (F) and by FISH assay (G). Scale bars: 200 μm. All experiments were carried out with n = 3 biological replicates. All data in the graphs were presented as mean ± SD. *P < 0.05, **P < 0.01, ***P < 0.001.

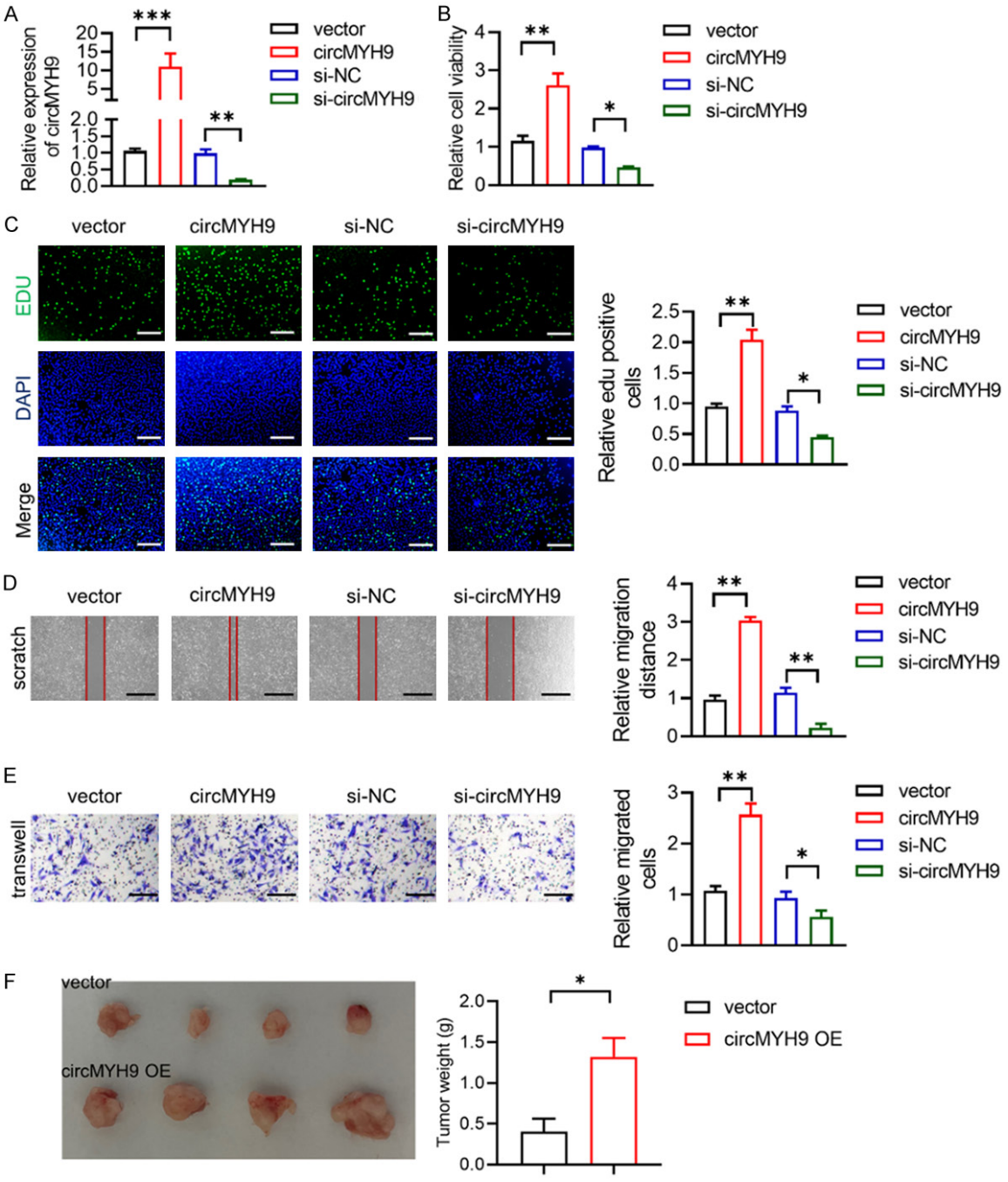

Figure 2. CircMYH9 functioned as an oncogene in HCC cells. (A) The expression of circMYH9 was evaluated by qRT-PCR in Huh-7 cells transfected with si-NC or si-circMYH9 (for circMYH9 knockdown) and transfected with LV-vector or LV-circMYH9 (for circMYH9 overexpression). (B, C) The effect of si-circMYH9 and LV-circMYH9 on the proliferation of Huh-7 cells by CCK8 assay (B) and by EDU staining assay (C). (D) Wound healing assays of Huh-7 cells transfected with si-circMYH9 or LV-circMYH9. Scale bars: 200 μm. (E) Transwell assays of Huh-7 cells transfected with si-circMYH9 or LV-circMYH9. Scale bars: 100 mm. (F) Xenograft tumors derived from circMYH9-overexpressing Huh-7 cells were significantly larger than those derived from vector transfected Huh-7 cells. All experiments were carried out with n = 3 biological replicates. All data in the graphs were presented as mean ± SD. *P < 0.05, **P < 0.01, ***P < 0.001.

downregulated circRNAs were identified in these two GEO databases (**Figure 1C**). We then analyzed the enriched pathways associated with these differentially expressed circRNAs. The data showed that differentially expressed circRNAs were involved in the metabolism of

mRNA and mRNA splicing pathways (**Figure 1D**). Among the 14 upregulated circRNAs, circMYH9, also known as hsa_circ_0092283, was one of the highly expressed circRNAs in HCC and was chosen for further study. circMYH9 was formed from intron 37 in the MYH9 gene (**Figure 1E**), and its expression was higher in HCC samples than in non-tumor tissues, as determined by qRT-PCR and FISH assay (**Figure 1F** and **1G**).

The oncogenic role of circMYH9 in HCC

To determine the functional importance of circMYH9 upregulation in HCC tumorigenesis, we examined the effect of altered circMYH9 expression in the growth of HCC cells. The successful overexpression or knockdown of circMYH9 in Huh-7 cells after transfection was verified by qRT-PCR (**Figure 2A**). CCK8 assay was first carried out to determine the effect of circMYH9 on cell viability, and we found that circMYH9 overexpression could induce cell proliferation, while circMYH9 knockdown reduced the cell viability (**Figure 2B**). Consistently, the expression of cell cycle-related proteins (Cyclin D1, Cyclin E2) in Huh-7 cells was significantly enhanced by circMYH9 overexpression, whereas it was reduced by circMYH9 knockdown (**Figure 2C**). Likewise, EDU staining showed that cell proliferation was significantly promoted by circMYH9 overexpression, while it was reduced by circMYH9 knockdown (**Figure 2C**). Furthermore, we studied the effect of circMYH9 on the motility of HCC cells by using wound healing assay and transwell assay. The results indicated that circMYH9 overexpression enhanced, while circMYH9 knockdown suppressed, the migration and invasion of Huh-7 cells (**Figure 2D** and **2E**). Importantly, we used xenograft tumor model to validate the oncogenic role of circMYH9 in HCC. Xenograft tumor was generated by subcutaneous injection of Huh-7 cells expressing vector or circMYH9 plasmid in nude mice. We observed significantly larger tumors derived from circMYH9 overexpressing cells than from control vector-expressing cells (**Figure 2F**). Collectively, these results suggested the oncogenic role of circMYH9 in HCC.

CircMYH9 binds to EIF4A3

Having determined the role of circMYH9 in HCC tumor growth, we sought to elucidate the molecular mechanism that mediated circMYH9 activity. Since circRNAs could act as a protein sponge [16], we employed CircInteractome (https://circinteractome.nia.nih.gov/) to predict the potential circMYH9 binding proteins, and we identified EIF4A3 as the only candidate protein containing circMYH9 binding site (**Figure 3A**). EIF4A3 has been known to function in mRNA surveillance pathway and spliceosome according to KEGG pathway analysis (**Figure 3B**), suggesting that EIF4A3 may be important in the process of mRNA regulation. We then confirmed the interaction between circMYH9 and EIF4A3 by using RNA pull-down assay and RNA immunoprecipitation (RIP) assay. As expected, EIF4A3 could be pulled down by circMYH9, as EIF4A3 was detected in the circMYH9 precipitated complex (**Figure 3C**). In consistent with this, circMYH9 was detected in the immunoprecipitated complex of EIF4A3 (**Figure 3D** and **3E**). We also used immunofluorescence staining to show that circMYH9 could co-localize with EIF4A3 in Huh-7 cells (**Figure 3F**). Taken together, these results demonstrated that circMYH9 could bind to EIF4A3.

To explore the functional relationship between EIF4A3 and circMYH9 in HCC, we evaluated the effect of circMYH9 overexpression in EIF4A3 knocked down Huh-7 cells. CCK8 assay showed that EIF4A3 knockdown could markedly reduce the viability of HCC cells, even though circMYH9 was overexpressed (**Figure 4A**). Similar results were obtained by EDU staining assay, in which cell proliferation was significantly reduced upon EIF4A3 knockdown, even in the presence of circMYH9 overexpression (**Figure 4B**). Furthermore, wound healing assay and transwell assay demonstrated that the migration and invasion of HCC cells were reduced in EIF4A3 knockdown cells (**Figure 4C** and **4D**). Together, these data suggested that EIF4A3 was required for circMYH9-regulated activities in HCC. Therefore, we speculated that circMYH9 functioned as an oncogene via binding to EIF4A3.

circMYH9 regulated KPNA2 level through recruiting EIF4A3 at the post-transcriptional level

We next aimed to delineate how EIF4A3 exerted its effect in mediating circMYH9's activity. According to the bioinformatics analysis of the co-expression network of EIF4A3 in human cancers, there were 24 EIF4A3 co-expressed genes in HCC. These genes were enriched in such biological pathways as oncogenic pathway and cell cycle pathway (**Figure 5A**). Gene

A

CircRNA	Tag Name	% Identity	Alignment Length	Mismatches	Gap Openings	Tag Start	Tag End	CircRNA Start	CircRNA End
circMYH9	HHLE2_769282_eIF4AIII_rep2_769282_1_36	100	36	0	0	1	36	39	74

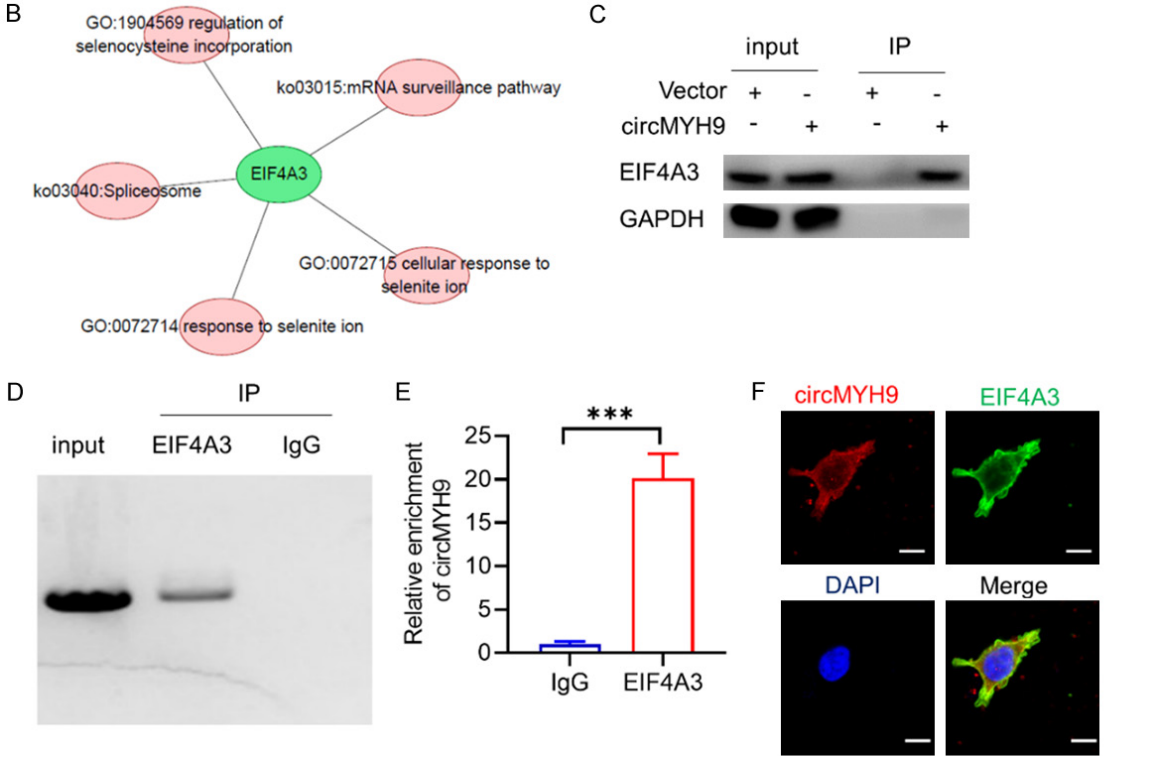

Figure 3. circMYH9 interacted with EIF4A3. A. Potential binding site between EIF4A3 and circMYH9 predicted by CircInteractome. B. Gene ontology analysis and KEGG pathway analysis of EIF4A3. C. RNA pull-down assay was used to determine the interaction between EIF4A3 and circMYH9. D and E. RIP assay was applied to verify the binding of EIF4A3 to circMYH9. F. FISH assays showed the co-localization of EIF4A3 and circMYH9 in Huh-7 cells. Scale bars: 20 μm. All experiments were carried out with n = 3 biological replicates. All data in the graphs were presented as mean ± SD. ***P < 0.001.

ontology analysis also showed that the molecular function of these genes was enriched in protein binding, and the biological process was enriched in the negative regulation of apoptotic process (**Figure 5B** and **5C**). Among the EIF4A3 co-expressed genes, KPNA2 was one of the top genes (**Figure 5D**), suggesting the likelihood of the functional association between EIF4A3 and KPNA2. Hence, we carried out a RIP assay and verified the interaction between EIF4A3 and KPNA2 mRNA (**Figure 5E**). RIP assay also demonstrated that the enrichment of KPNA2 mRNA could be reduced by circMYH9 knockdown (**Figure 5F**). As expected, the stability of KPNA2 mRNA was reduced by knocking down of circMYH9 in Huh-7 cells (**Figure 5G**). Furthermore, the expression of EIF4A3 was suppressed upon circMYH9 knockdown, and the stability of KPNA2 mRNA was decreased by EIF4A3 knockdown (**Figure 5G**).

KPNA2 knockdown reversed the effects caused by circMYH9 overexpression in HCC cells

We further validated whether the KPNA2 expression could be regulated by circMYH9 in HCC cells. The results demonstrated that the level of KPNA2 was enhanced by circMYH9 overexpression and was reduced by circMYH9 knockdown (**Figure 6A**). In addition, we explored the association in expression between KPNA2 and circMYH9 in HCC tumor samples by qRT-PCR. Like circMYH9, KPNA2 level was also significantly upregulated in HCC tissues (**Figure 6B**). Pearson's correlation analysis demonstrated that circMYH9 level was positively correlated with KPNA2 level (**Figure 6C**). Finally, rescue experiments were carried out to explore the importance of KPNA2 in circMYH9-regulated proliferation, migration, and invasion of

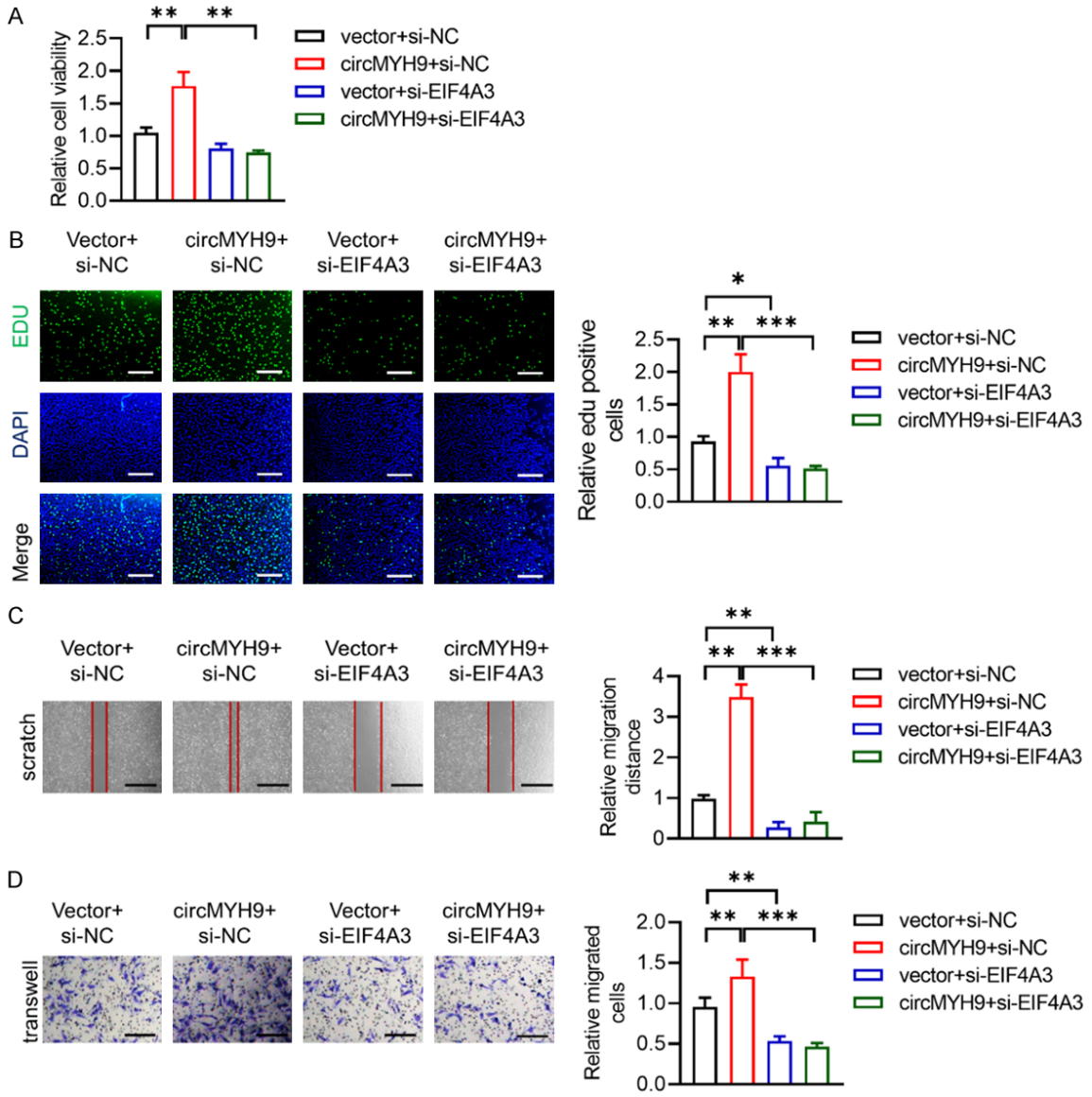

Figure 4. The oncogenic role of EIF4A3 in HCC cells. (A, B) The effect of EIF4A3 knockdown by si-EIF4A3 in the absence or presence of circMYH9 on the viability of Huh-7 cells determined by CCK8 assays (A) and by EDU staining assays (B). (C) Wound healing assays of Huh-7 cells transfected with si-EIF4A3 under LV-circMYH9-expressing condition. Scale bars: 200 μm. (D) Transwell assays of cells transfected with si-EIF4A3 under LV-circMYH9-expressing condition. Scale bars: 100 μm. All experiments were carried out with n = 3 biological replicates. All data in the graphs were presented as mean ± SD. *P < 0.05, **P < 0.01, ***P < 0.001.

HCC cells. KPNA2 knockdown in Huh-7 cells could remarkably reduce cell viability that was enhanced by circMYH9 overexpression, as determined by CCK8 assay (**Figure 6D**). EDU staining assay showed the similar results (**Figure 6E**). A wound healing assay and transwell assay demonstrated that the migration and invasion of Huh-7 cell were reduced in the EIF4A3-knockdown group (**Figure 6F** and **6G**). In conclusion, KPNA2 knockdown reversed the enhanced proliferation, migration, and invasion of HCC cells caused by circMYH9 overexpression.

Discussion

Accumulating evidence has revealed that non-coding RNAs play critical role in tumorigenesis. circRNAs are especially important because of their stable structure which is different from other non-coding RNAs [17]. circRNAs could act as microRNA sponges, protein sponges or scaf-

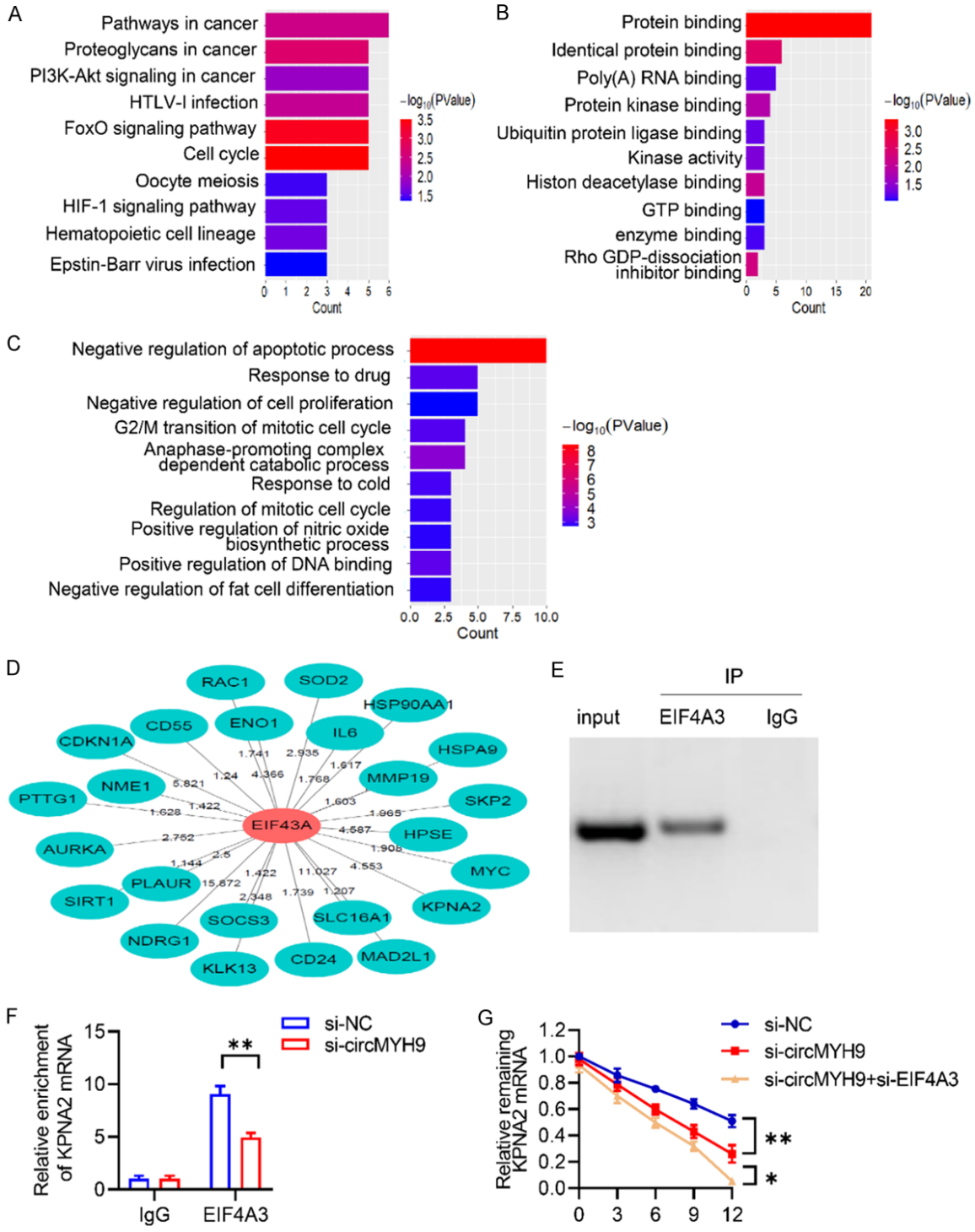

Figure 5. circMYH9 increased KPNA2 mRNA stability through recruiting EIF4A3. (A) KEGG analysis of EIF4A3 co-expressed genes in HCC (DOID:3459). (B, C) The molecular function (B) and biological process (C) of EIF4A3 co-expressed genes in HCC by Gene ontology analysis. (D) EIF4A3 co-expressed partners. (E) Binding of EIF4A3 to KPNA2 by RIP assays. (F) Interaction between EIF4A3 and KPNA2 after circMYH9 knockdown by RIP assays. (G) The mRNA stability of KPNA2 in Huh-7 cells was evaluated by qRT-PCR after actinomycin D treatment. All experiments were carried out with n = 3 biological replicates. All data in the graphs were presented as mean ± SD. **P < 0.01, ***P < 0.001.

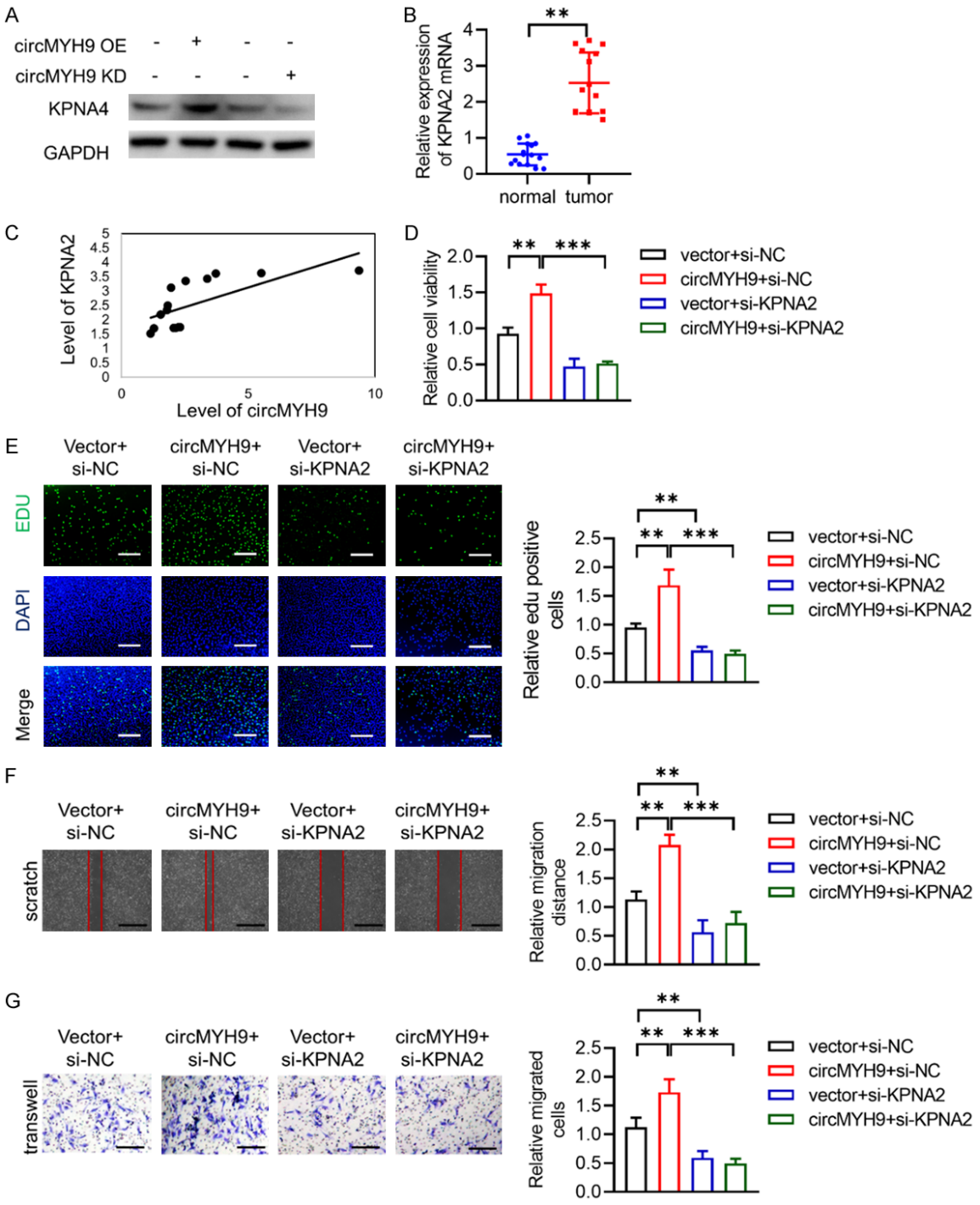

Figure 6. KPNA2 knockdown reversed the enhanced proliferation, migration, and invasion of HCC cells by circMYH9 overexpression. (A) The effect of si-circMYH9 and LV-circMYH9 on the expression of KPNA2 in Huh-7 cells by Western blotting. (B) Upregulation of KPNA2 expression in tumor tissues. (C) Correlation between the expression of circMYH9 and KPNA2 by Pearson's correlation analysis. (D, E) The effect of si-KPNA2 on the viability of LV-circMYH9-expressing cells determined by CCK8 assays (D) and by EDU staining assays (E). (F) si-KPNA2 reversed the enhanced migration of circMYH9-overexpressing Huh-7 cells determined by wound healing assays. Scale bar: 100 μm. (G) si-KPNA2 reversed the enhanced invasion of circMYH9-overexpressing Huh-7 cells determined by transwell assays. Scale bar: 100 μm. All experiments were carried out with n = 3 biological replicates. All data in the graphs were presented as mean ± SD. *P < 0.05, **P < 0.01, ***P < 0.001.

folds, translation templates, gene expression regulators to regulate the development of HCC [18].

In our study, we identified a novel circRNA, circMYH9, whose expression was upregulated in HCC from bioinformatics analyses using GEO databases (GSE138734 and GSE122482) and experimentally validated that the level of circMYH9 was increased in HCC tissues. circMYH9 was initially reported to promote colorectal cancer growth by regulating serine metabolism and redox homeostasis in a p53-dependent manner [19]. Here, we showed that circMYH9 could promote HCC cell proliferation, migration, and invasion. Since circRNAs can sponge miRNAs, bind to RBPs, and regulate gene transcription and translation [16, 20], we focused on the RBPs ability of circMYH9 in our study as the differentially expressed circRNAs we identified were associated with metabolism of mRNA and mRNA splicing pathways. We were also the first to demonstrate the interaction between circMYH9 and EIF4A3. EIF4A3 has been reported as a nuclear matrix protein and functions as a core element of the exon junction complex (EJC), which is involved in RNA surveillance pathway [21]. Furthermore, EIF4A3 can induce the progression of multiple human cancers, including HCC [22], pancreatic cancer [23], glioblastoma [24], and ovarian cancer [25]. In breast cancer, upregulation of EIF4A3 is correlated with poor prognosis [26].

Among the 24 EIF4A3 co-expressed genes identified in HCC by our co-expression network analysis, we chose KPNA2 for further analysis since other genes acted as tumor suppressors. Karyopherin α2 (KPNA2) is a component of the nuclear transporter and transported tumor-associated proteins [27]. Many studies have indicated that KPNA2 is overexpressed in various cancers, including non-small cell lung cancer, epithelial ovarian carcinoma, colorectal cancer, and HCC [28]. Especially, the expression of KPNA2 was associated with the survival of HCC patients. Therefore, KPNA2 could act as a potential therapeutic target for the treatment of HCC. In our study, we also found KPNA2 level was increased in HCC tissues and was positively correlated with the level of circMYH9. The RNA pull-down assay and RIP assay confirmed that EIF4A3 could bind to KPNA2 mRNA and increase KPNA2 mRNA stability. KPNA2 knockdown reversed the enhanced proliferation, migration, and invasion of HCC cells by circMYH9 overexpression.

In conclusion, our study revealed that circMYH9 was upregulated in HCC and could promote HCC progression by binding to EIF4A3 to increase KPNA2 mRNA stability. These findings suggested that circMYH9 could serve as a novel potential target for the diagnose and treatment of HCC.

Acknowledgements

The study was supported by grants from the National Natural Science Foundation of China (Grant no. 81972675). The work was also supported in part by the Program for Development of Innovative Research Teams in the First Affiliated Hospital of NJMU, the Priority Academic Program of Jiangsu Higher Education Institutions. This study was also supported by Basic Research Program of Jiangsu Province (BK20221415).

Informed consent was obtained from each patient, and ethical approval was granted by the Ethics Committee of The First Affiliated Hospital of Nanjing Medical University.

Disclosure of conflict of interest

None.

Address correspondence to: Drs. Han Zhuo and Zhongming Tan, Hepatobiliary Center, The First Affiliated Hospital of Nanjing Medical University, Nanjing, Jiangsu, P. R. China. Tel: +86-025-6830-3230; Fax: +86-25-8371-4511; E-mail: han12175@hotmail.com (HZ); Tel: +86-025-68303215; Fax: +86-25-8371-4525; E-mail: tanzhongming@njmu.edu.cn (ZMT)

References

[1] Llovet JM, Kelley RK, Villanueva A, Singal AG, Pikarsky E, Roayaie S, Lencioni R, Koike K, Zucman-Rossi J and Finn RS. Hepatocellular carcinoma. Nat Rev Dis Primers 2021; 7: 6.

[2] Armengol C, Sarrias MR and Sala M. Hepatocellular carcinoma: present and future. Med Clin (Barc) 2018; 150: 390-397.

[3] Forner A, Reig M and Bruix J. Hepatocellular carcinoma. Lancet 2018; 391: 1301-1314.

[4] Huang Z, Xia H, Liu S, Zhao X, He R, Wang Z, Shi W, Chen W, Kang P, Su Z, Cui Y, Yam JWP and Xu Y. The mechanism and clinical significance of circular rnas in hepatocellular carcinoma. Front Oncol 2021; 11: 714665.

[5] Jeck WR, Sorrentino JA, Wang K, Slevin MK, Burd CE, Liu J, Marzluff WF and Sharpless NE. Circular RNAs are abundant, conserved, and associated with ALU repeats. RNA 2013; 19: 141-157.
[6] Arnaiz E, Sole C, Manterola L, Iparraguirre L, Otaegui D and Lawrie CH. CircRNAs and cancer: biomarkers and master regulators. Semin Cancer Biol 2019; 58: 90-99.
[7] Li Z, Huang C, Bao C, Chen L, Lin M, Wang X, Zhong G, Yu B, Hu W, Dai L, Zhu P, Chang Z, Wu Q, Zhao Y, Jia Y, Xu P, Liu H and Shan G. Exon-intron circular RNAs regulate transcription in the nucleus. Nat Struct Mol Biol 2015; 22: 256-264.
[8] Zhang Y, Zhang XO, Chen T, Xiang JF, Yin QF, Xing YH, Zhu S, Yang L and Chen LL. Circular intronic long noncoding RNAs. Mol Cell 2013; 51: 792-806.
[9] Jeck WR and Sharpless NE. Detecting and characterizing circular RNAs. Nat Biotechnol 2014; 32: 453-461.
[10] Lu Z, Filonov GS, Noto JJ, Schmidt CA, Hatkevich TL, Wen Y, Jaffrey SR and Matera AG. Metazoan tRNA introns generate stable circular RNAs in vivo. RNA 2015; 21: 1554-1565.
[11] Okholm TLH, Nielsen MM, Hamilton MP, Christensen LL, Vang S, Hedegaard J, Hansen TB, Kjems J, Dyrskjot L and Pedersen JS. Circular RNA expression is abundant and correlated to aggressiveness in early-stage bladder cancer. NPJ Genom Med 2017; 2: 36.
[12] Abdelmohsen K, Panda AC, Munk R, Grammatikakis I, Dudekula DB, De S, Kim J, Noh JH, Kim KM, Martindale JL and Gorospe M. Identification of HuR target circular RNAs uncovers suppression of PABPN1 translation by circPABPN1. RNA Biol 2017; 14: 361-369.
[13] Legnini I, Di Timoteo G, Rossi F, Morlando M, Briganti F, Sthandier O, Fatica A, Santini T, Andronache A, Wade M, Laneve P, Rajewsky N and Bozzoni I. Circ-ZNF609 is a circular RNA that can be translated and functions in myogenesis. Mol Cell 2017; 66: 22-37, e29.
[14] Li J, Hu ZQ, Yu S, Mao L, Zhou Z, Wang P, Gong Y, Su S, Zhou J, Fan J, Zhou SL and Huang X. CircRPN2 inhibits aerobic glycolysis and metastasis in hepatocellular carcinoma. Cancer Res 2022; 82: 1055-1069.
[15] Zhang J, Xu HD, Xing XJ, Liang ZT, Xia ZH and Zhao Y. CircRNA_069718 promotes cell proliferation and invasion in triple-negative breast cancer by activating Wnt/beta-catenin pathway. Eur Rev Med Pharmacol Sci 2019; 23: 5315-5322.
[16] Jiang MP, Xu WX, Hou JC, Xu Q, Wang DD and Tang JH. The emerging role of the interactions between circular RNAs and RNA-binding proteins in common human cancers. J Cancer 2021; 12: 5206-5219.
[17] Sole C and Lawrie CH. Circular RNAs and cancer: opportunities and challenges. Adv Clin Chem 2020; 99: 87-146.
[18] Ma Y, Zheng L, Gao Y, Zhang W, Zhang Q and Xu Y. A comprehensive overview of circRNAs: emerging biomarkers and potential therapeutics in gynecological cancers. Front Cell Dev Biol 2021; 9: 709512.
[19] Liu X, Liu Y, Liu Z, Lin C, Meng F, Xu L, Zhang X, Zhang C, Zhang P, Gong S, Wu N, Ren Z, Song J and Zhang Y. CircMYH9 drives colorectal cancer growth by regulating serine metabolism and redox homeostasis in a p53-dependent manner. Mol Cancer 2021; 20: 114.
[20] Chen LL. The expanding regulatory mechanisms and cellular functions of circular RNAs. Nat Rev Mol Cell Biol 2020; 21: 475-490.
[21] Ye J, She X, Liu Z, He Z, Gao X, Lu L, Liang R and Lin Y. Eukaryotic initiation factor 4A-3: a review of its physiological role and involvement in oncogenesis. Front Oncol 2021; 11: 712045.
[22] Tian M, Cheng H, Wang Z, Su N, Liu Z, Sun C, Zhen B, Hong X, Xue Y and Xu P. Phosphoproteomic analysis of the highly-metastatic hepatocellular carcinoma cell line, MHCC97-H. Int J Mol Sci 2015; 16: 4209-4225.
[23] Xia Q, Kong XT, Zhang GA, Hou XJ, Qiang H and Zhong RQ. Proteomics-based identification of DEAD-box protein 48 as a novel autoantigen, a prospective serum marker for pancreatic cancer. Biochem Biophys Res Commun 2005; 330: 526-532.
[24] Wang R, Zhang S, Chen X, Li N, Li J, Jia R, Pan Y and Liang H. EIF4A3-induced circular RNA MMP9 (circMMP9) acts as a sponge of miR-124 and promotes glioblastoma multiforme cell tumorigenesis. Mol Cancer 2018; 17: 166.
[25] Li Y, Ren S, Xia J, Wei Y and Xi Y. EIF4A3-induced circ-BNIP3 aggravated hypoxia-induced injury of H9c2 cells by targeting miR-27a-3p/BNIP3. Mol Ther Nucleic Acids 2020; 19: 533-545.
[26] Wang X, Chen M and Fang L. hsa_circ_006-8631 promotes breast cancer progression through c-Myc by binding to EIF4A3. Mol Ther Nucleic Acids 2021; 26: 122-134.
[27] Radu A, Blobel G and Moore MS. Identification of a protein complex that is required for nuclear protein import and mediates docking of import substrate to distinct nucleoporins. Proc Natl Acad Sci U S A 1995; 92: 1769-1773.
[28] Han Y and Wang X. The emerging roles of KPNA2 in cancer. Life Sci 2020; 241: 117140.